Single Chain Fv Antibodies against the 25−35 Aβ Fragment Inhibit Aggregation and Toxicity of Aβ42[†]

Andleeb Zameer, Philip Schulz, Min S. Wang, and Michael R. Sierks*

Department of Chemical and Materials Engineering, Arizona State University, Tempe, Arizona 85287-6006

Received March 27, 2006; Revised Manuscript Received July 17, 2006

ABSTRACT: Alzheimer's disease (AD) is characterized by the deposition of amyloid-β (Aβ) protein in the brain. Immunization studies have demonstrated that anti-Aβ antibodies reduce Aβ deposition and improve clinical symptoms seen in AD. However, conventional antibody-based therapies risk an inflammatory response that can result in meningoencephalitis and cerebral hemorrhage. Here we report on the development of human-based single chain variable domain antibody fragments (scFvs) directed against the Aβ 25−35 region as potential therapeutics for AD that do not risk an inflammatory response. The 25−35 region of Aβ represents a promising therapeutic target since it promotes aggregation and is highly toxic. Two scFvs with differing affinities for Aβ were studied, and both inhibited aggregation of Aβ42 as determined by thioflavin T binding assay and atomic force microscopy analysis and blocked Aβ-induced toxicity toward human neuroblastoma SH-SY5Y cells as determined by MTT and LDH release assays. These results provide additional evidence that scFvs against Aβ provide an attractive alternative to more conventional antibody-based therapeutics for controlling aggregation and toxicity of Aβ.

Alzheimer's disease (AD)[1] is a progressive neurodegenerative disorder characterized clinically by memory and cognitive dysfunction and the presence of senile plaques and neurofibrillary tangles (NFT) (*1*). Although sporadic Alzheimer's disease is rare in individuals younger than 60 years of age, the incidence increases with age, affecting up to 40% of people 85 years of age and older (*2*). AD affects approximately 15 million people worldwide, and the number of affected individuals in the United States and Europe is expected to triple by the year 2050 (*3*, *4*), underscoring the need to devise effective treatments or preventive interventions. The senile plaques are composed of β-amyloid (Aβ), a cleavage product of amyloid precursor protein (APP), whereas NFTs contain aberrantly phosphorylated tau, a microtubule-associated protein (*2*). Abundant evidence now suggests that a key event in AD pathogenesis is the conversion of the Aβ peptide from soluble to aggregated forms in the brain (*5*). Aβ is predominantly 40−42 amino acids in length and is a normal, soluble proteolytic product of the APP, a large integral membrane protein expressed at high levels in the brain (*6*). Studies of various mutations in the APP and presenilin genes, all of which result in early onset, autosomal dominant, familial AD, share a common feature: they all increase Aβ production or increase the ratio of Aβ42/Aβ40 (*7*, *8*). Aβ42 has a higher tendency to misfold and aggregate compared to Aβ40, leading to synaptic and neuritic compromise and glial activation, contributing toward the neuropathology seen in AD (*9*). While early evidence implicated insoluble fibrillar forms of Aβ with neurotoxicity (*10*, *11*), recent studies suggest that other morphologies of Aβ, including protofibrils and soluble oligomers, are more neurotoxic (*12*−*15*). Additionally, soluble Aβ concentrations correlate better with AD pathology than fibrils (*16*−*18*), further supporting a key role for soluble morphologies of Aβ in AD.

A number of different treatment strategies for AD have been investigated including reducing Aβ synthesis by targeting enzymes that process APP to Aβ peptide (*19*), inhibiting or reducing Aβ aggregation (*20*−*22*), increasing clearance of Aβ from the brain (*20*, *23*, *24*), and reducing inflammation associated with Aβ deposition (*25*, *26*). Clearance of Aβ by active immunization with aggregated Aβ inhibited fibril formation and improved memory deficits in animal models of AD and also human patients (*27*, *28*). Administration of anti-Aβ antibodies reduced amyloid deposition, decreased the plaque burden, and reversed memory deficits in animal studies (*29*−*33*). Both active and passive immunization with Aβ results in activated microglial cells and phagocytosis (*33*−*35*). However, intracranial administration of an anti-Aβ F(ab′)$_2$ fragment was as effective as administration of the entire antibody in reducing Aβ cortical load in a mouse model of AD (*33*, *36*), indicating that non-Fc-mediated processes are also involved in Aβ clearance. While Aβ vaccination trials in humans were quickly halted due to signs of aseptic meningoencephalitis in several patients (*37*), follow-up studies did not show a correlation between anti-Aβ antibody titers and the incidence and severity of encephalomyelitis (*38*). Potentially dangerous effects of Aβ immunization strategies including increase in cerebral microhemorrhaging and inflammation have been reported in human and animal studies (*37*, *39*, *40*). Therefore, single

[†] This work was supported in part by a grant from the NIH (AG17984).

* Corresponding author. Phone: 480-965-2828. Fax: 480-965-0037. E-mail: Sierks@asu.edu.

[1] Abbreviations: AD, Alzheimer's disease; Aβ, β-amyloid; scFv, single chain variable fragment; ThT, thioflavin T; AFM, atomic force microscopy; MTT, 3-(4,5-dimethylthiazol-2-yl)-2,5-diphenyltetrazolium bromide; LDH, lactate dehydrogenase.

10.1021/bi060601o CCC: $33.50
Published on Web 09/02/2006

chain variable domain antibody fragments (scFvs) represent a promising therapeutic approach for inhibiting toxic Aβ aggregation since they do not contain the Fc region responsible for activating the complement response leading to inflammation. The lack of Fc region at least removes one potential risk factor associated with antibody-based therapy.

The 25−35 fragment of Aβ by itself is highly toxic to neurons (*41*−*43*), promotes aggregation of full-length Aβ (*44*), and accumulates in AD brains in a racemized form (L- to D-Ser 26) (*45*). Racemization of Ser and Asp occurs as part of the normal aging process (*41*), so the 25−35 fragment can be produced in aged AD brains when the soluble racemized Aβ40 is proteolytically cleaved (*45*). Here we report the production of scFvs against the Aβ 25−35 fragment from naive human phage display antibody libraries. We show that these scFvs are effective in inhibiting the aggregation of Aβ42 in vitro as well as reducing Aβ42-induced neurotoxicity in cell culture studies. These results suggest that scFvs may be part of a potential therapeutic for treating AD since they can inhibit aggregation and reduce neuronal toxicity of Aβ42 without risking an increased inflammatory response.

EXPERIMENTAL PROCEDURES

Bio-Panning Using the Phage Display Library. A naive human single chain variable domain (scFv) phage display library, Tomlinson I and J (*46*), was obtained from the Medical Research Council (MRC, Cambridge, U.K.). ScFv selection was performed using three rounds of panning essentially as described earlier (*47*) with slight modifications. Amine-binding 96-well microtiter plates (Corning) were coated with 10 μg/mL Aβ 25−35 fragment (Biosource) in PBS (10 mM phosphate, 150 mM NaCl, pH 9.0) overnight at 4 °C. Plates were blocked with 2% milk powder in PBS (10 mM phosphate, 150 mM NaCl, pH 7.4) for at least 2 h at room temperature. An aliquot of 10^{12} phage units from the naive library was incubated with the peptide. Plates were thoroughly washed with PBS, pH 7.4, plus 0.1% Tween-20 (Sigma) solution to remove any unbound phage. Bound phage was eluted with trypsin (Sigma) in PBS (50 μL of trypsin stock solution in 50 mM Tris-HCl, pH 7.4, and 1 mM $CaCl_2$ added to 450 μL of PBS, pH 7.4). *Escherichia coli TG1* strain (provided by the MRC) was infected with the eluted phage, serially diluted, and plated on agar plates containing 100 μg/mL ampicillin to determine the phage titers. Eluted phage was also amplified in *E. coli TG1* in the presence of KM13, a protease-cleavable helper phage as described elsewhere (*46*). Amplified phage was purified using the polyethylene glycol (MW 6000)/NaCl precipitation method as described (*47*) and used for further rounds of selection.

Production of Soluble ScFv and ELISA. Eluted phage from the third round of selection was used to infect *E. coli HB2151*, a nonsuppressor strain used for production of soluble scFv antibody. Individual clones were grown essentially as described (*47*). ScFv expression was induced by adding 1 mM isopropyl β-D-thiogalactoside (IPTG). The plates were centrifuged at 1800*g* for 10 min, and the supernatant was used to screen for positive scFvs using ELISA. Amine-binding 96-well ELISA plates (Corning) were coated with 10 μg per well of Aβ 25−35 fragment in PBS, pH 9.0, overnight at 4 °C. ScFv supernatant was added to each well and incubated for 2 h at room temperature. Anti-myc 9E10 antibody (Santa Cruz Biotechnology) was added to the wells followed by a secondary antibody, goat anti-mouse IgG HRP conjugated (Santa Cruz Biotechnology). TMB substrate (Sigma) was added to the wells, and the reaction was stopped after 30 min by addition of 50 μL of 2 N H_2SO_4. Absorbance was read as a difference between OD 450 nm and OD 650 nm on a Wallac 1420 plate reader (Perkin-Elmer). Clones showing the highest absorbance based on ELISA were selected for further studies.

ELISA was performed with purified scFvs to detect binding to Aβ40, Aβ42, and the Aβ 25−35 fragment. Wells were coated with 20 μM antigen concentration in PBS, pH 9.0, overnight at 4 °C. Purified scFv (1 μM concentration) was added to the wells. Values were calculated as the average of two different experiments after subtracting out control wells without antigen.

Production and Purification of ScFvs. For production of soluble scFv, selected clones were grown in a 5 L culture volume using a BIOFLOW 110 fermentor (New Brunswick Scientific) under 35% dissolved oxygen concentration (dO_2), agitation at 250 rpm, and 30 °C. The supernatant was obtained by spinning the culture, and the cell pellet was stored at −20 °C until periplasmic fraction preparation. Briefly, the cell pellet was thawed on ice and treated with 30 mM Tris-HCl, pH 8.0, 20% sucrose, and 1 mM ethylenediaminetetraacetic acid (EDTA) for 20 min on ice. Cells were spun down to obtain supernatant I. The cell pellet was treated again with 5 mM $MgSO_4$ on ice for 20 min followed by centrifugation to obtain supernatant II. Supernatants I and II were pooled together containing the periplasmic fraction. The supernatant and periplasmic fractions (supernatants I and II) were combined, passed through a 0.2 μm filter (Whatman), and concentrated using a tangential flow filter (Mllipore) using a 10 kDa cutoff filter (Millipore). Concentrated samples were dialyzed overnight at 4 °C against PBS and purified using a protein A column as described (*48*). The eluted fractions were analyzed by SDS−PAGE on a 15% polyacrylamide gel and also by Western blot using anti-myc 9E10 antibody (Santa Cruz Biotechnology).

Sequencing the Selected Clones. Selected clones were analyzed further by nucleic acid sequencing. Phagemid DNA was purified with the Qiagen kit (Qiagen), according to the manufacturer's protocol, and sequenced at the Arizona State University DNA laboratory facility. Two sequencing primers were used: the heavy chain primer 5′-CGA CCC GCC ACC GCC GCT G-3′ and the light chain primer 5′-CTA TGC GGC CCC ATT CA-3′.

Surface Plasmon Resonance Analysis. Affinity measurements were performed using a BIAcore X biosensor (BIAcore Inc., Uppsala, Sweden). A CM5 sensor chip was activated using an equimolar mix of NHS (*N*-hydroxysuccinimide) and EDC [*N*-ethyl-*N*′-(dimethylaminopropyl)-carbodiimide], coupled with 20 μg/mL Aβ40 in pH 4.8 sodium acetate buffer, and then blocked with ethanolamine. The Aβ 25−35 fragment was immobilized onto a separate CM5 sensor chip. ScFv samples were diluted in HBS-EP buffer (BIAcore). The association and dissociation rate constants (k_a and k_d, respectively) were calculated using the following concentrations for D4 (260, 200, 100, and 50 nM for Aβ40 and 4700, 2800, 1900, 960, and 350 nM for Aβ

25−35) and B6 (1900, 950, 475, 260, and 200 nM for Aβ40 and 3000, 2000, 1000, and 500 nM for Aβ25−35) with HBS-EP as a running buffer at a flow rate of 30 μL/min. The association and dissociation constants for the scFv were calculated by fitting the data to a single binding model. Kinetic parameters were evaluated using BIAevaluation 3.1 software (BIAcore).

Fluorescence-Based Aggregation Assay. Thioflavin (ThT) associates rapidly with aggregated fibrils of Aβ40/42 peptide, giving rise to an excitation maximum at 450 nm and enhanced emission at 482 nm (*49*). Aβ42 peptide (Biosource) was dissolved in 1,1,1,3,3,3-hexafluoro-2 propanol (HFIP) (Sigma); aliquots were removed, air-dried, and stored at −20 °C until further use. Each aliquot was further dissolved in 100% dimethyl sulfoxide (DMSO) (Mallinckrodt) at a concentration of 221.5 μM. For aggregation purposes, Aβ42 stock in DMSO was diluted to 20 μM concentration in PBS, pH 7.4, and incubated at 37 °C in 0.5 mL Eppendorf tubes. To study the effects of scFvs on aggregation, Aβ42 was mixed with equimolar concentrations of each of the two scFvs to a final concentration of 20 μM. Aggregation at different time intervals was measured by removing 10 μL aliquots of the sample and adding them to 2 mL of 5 μM ThT solution (50 mM phosphate buffer, pH 6.5). Fluorescence intensity was measured at an excitation wavelength of 450 nm and an emission wavelength of 482 nm using a Shimadzu PF-3501PC spectrofluorophotometer. Data were reported as the mean of three values determined by a time scan after subtracting the fluorescence with ThT alone.

Atomic Force Microscope (AFM) Imaging of Aggregates. AFM was used to analyze the morphology of the Aβ42 aggregates over time in the presence or absence of scFvs. Aliquots were removed from the samples and immediately spotted on freshly cleaved mica. After 2 min the mica was washed with 200 μL of deionized water, dried with compressed nitrogen, and completely air-dried under vacuum. Images were acquired in air using a multimode AFM nanoscope IIIA system (Veeco/Digital Instruments) operating in the tapping mode using silicon probes (Olympus).

Cytotoxicity Assays: MTT and LDH Release Assay. The human neuroblastoma cell line, SH-SY5Y, was obtained from the American Tissue Culture Collection. Cells were grown in medium containing 50% minimal essential medium (Invitrogen), 50% Ham's modification of F-12 (Invitrogen), 10% fetal bovine serum (Sigma), 1% MEM nonessential amino acids (Gibco), and a 1% mix of the antibiotics penicillin, streptomycin, and amphotericin antifungal (Gibco) in 5% CO_2 at 37 °C. Cells were plated in 96-well tissue culture treated plates (Corning) at approximately 10^5 cells per well in 100 μL of medium and incubated for 24 h to allow attachment to the bottom of the wells. Media were aspirated off and replaced with 100 μL of serum-free media. Samples of 20 μM Aβ42 alone or with the equimolar concentrations of scFv were incubated, and aliquots were removed at various time points. Aliquots were diluted with medium to a final concentration of 100 nM and added to the wells. Plates were incubated for an additional 48 h at 37 °C. Cell viability was determined using both MTT toxicity and LDH release assays. For the MTT assay, 10 μL of 5 mg/mL MTT [3-(4,5-dimethylthiazol-2-yl)-2,5-diphenyltetrazolium bromide] was added to each well and incubated for 3 h at 37 °C. Cells were briefly centrifuged and media aspirated off from the wells prior to adding dissolvent (0.1 N HCl in 2-propanol) to each well to dissolve the crystals. The absorbance was measured at 560 nm wavelength using a Victor Wallac multiwell plate reader (Gaithersburg, VA).

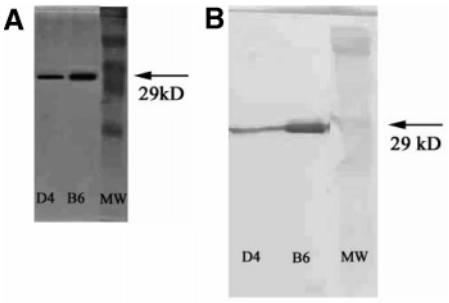

FIGURE 1: (A) SDS−15% PAGE gel stained with Coomassie blue showing purified B6 and D4 scFvs. Lanes: 1, D4 scFv; 2, B6 scFv; 3, standard molecular weight markers. (B) Western blot detection of scFv. Purified scFvs D4 and B6 were resolved on 15% SDS−PAGE and transferred to a nitrocellulose membrane. ScFv was immunodetected using an anti-myc 9E10 antibody. A 29 kDa band indicates the full size scFv. Lanes: 1, D4 scFv; 2, B6 scFv.

LDH release was measured using an LDH release toxicity kit (Sigma). Following the protocol provided by the manufacturer, cells were centrifuged, and 50 μL of media from each well was transferred to a fresh plate. An aliquot of 25 μL of the LDH assay mixture (equal volume of substrate, enzyme, and dye) was added to each of the wells, and the plate was incubated for 30 min at room temperature in the dark. The reaction was stopped by addition of $^1/_{10}$th volume of 1 N HCl to each well. Absorbance was measured as a difference between 490 and 690 nm wavelengths. For both MTT and LDH release assay, six wells were used for each sample, and each experiment was repeated three times. Cell viability and LDH release were determined by dividing the absorbance of treated wells by the absorbance of wells containing medium alone. Data were analyzed by using EXCEL software to calculate the standard deviation from the mean for each condition and plotted as a percentage of control values.

RESULTS

ScFvs against the Aβ 25−35 peptide were selected from a human naive phage display antibody library after three rounds of panning. The two clones with the highest ELISA values out of 96 screened, B6 and D4, were selected for further studies. Purified scFv from each clone showed the expected 29 kDa band on SDS−PAGE (Figure 1A), as verified by immunoblot using anti-myc 9E10 antibody (Figure 1B). Several minor smaller bands were also detected on the immunoblot, indicating some minor degradation of the scFv during purification. The B6 and D4 scFvs were analyzed by nucleic acid sequencing, and the deduced amino acid sequence is shown (Figure 2).

The affinities of the two scFvs to Aβ 25−35, Aβ40 and Aβ42, were determined by ELISA (Table 1). In addition, the association (k_a) and dissociation (k_d) rate constants and dissociation constants ($K_D = k_a/k_d$) of D4 and B6 for Aβ40 and the Aβ 25−35 fragment were also determined (Table 2). D4 shows higher affinity compared to B6 for Aβ40 (Table 2) whereas B6 has slightly higher affinity for the Aβ 25−35 fragment (Table 2), primarily due to difference in the respective k_a values.

MKYLLPTAAAGLLLLAAQPAMAEVQLLESGGGLVQPGGSLRLSCAASGFTFSSY------B6 ScFv------

MKYLLPTAAAGLLLLAAQPAMAEVQLLESGGGLVQPGGSLRLSCAASGFTFSSY------D4 ScFv-----

AMSWVRQAPGKGLEWVS***T***I***GTA***G***AY***T***A***YADSVKGRFTISRDNSKNTLYLQMNS-----B6 ScFv-----

AMSWVRQAPGKGLEWVS***YIDNT***G***SA***T***S***YADSVKGRFTISRDNSKNTLYLQMNS-----D4 ScFv-----

LRAEDTAVYYCAK***SAAT***FDYWGQGTLVTVSS*GGGGSGGGGSGGG*GSTDIQMTQ----B6 ScFv-----

LRAEDTAVYYCAK***ASAS***FDYWGQGTLVTVSS*GGGGSGGGGSGGG*GSTDIQMTQ----D4 ScFv-----

SPSSLSASVGDRVTITCRASQSISSYLNWYQQKPGKAPKLLIYAAS***A***LQSGVPLRF----B6 ScFv-----

SPSSLSASVGDRVTITCRASQSISSYLNWYQQKPGKAPKLLIYAAS***T***LQSGVPSRF----D4 ScFv-----

SGSGSGTDFTLTISSLQPEDFATYYCQQ***SYAG***P***T***TFGQGTKVEIKRAAAHHHHHH----B6 ScFv-----

SGSGSGTDFTLTISSLQPEDFATYYCQQ***SATN***P***S***TFGQGTKVEIKRAAAHHHHHH----D4 ScFv-----

GAAEQKLISEEDLNGAA* -------B6 ScFv---------

GAAEQKLISEEDLNGAA*--------D4 ScFv--------

FIGURE 2: Deduced amino acid sequence of the variable heavy chain (V_H) and variable light chain (V_L) region of anti-Aβ 25−35 scFvs B6 and D4 shown as an alignment. The linker sequence between the V_H and V_L is shown in italic and underlined. Variability between B6 and D4 residues are shown in bold and italics primarily located within the CDR regions of the heavy and light chain.

Table 1: Binding of D4 and B6 to Aβ40, Aβ42, and the Aβ 25−35 Fragment by ELISA

	Aβ 1−40	Aβ 1−42	Aβ 25−35
D4 scFv	0.687 ± 0.183	0.464 ± 0.122	0.572 ± 0.073
B6 scFv	1.881 ± 0.218	1.960 ± 0.277	1.874 ± 0.177

Table 2: Association, Dissociation, and Equilibrium Constants for ScFv Binding to Aβ40 and the Aβ 25−35 Fragment Determined by BIAcore Analysis

	K_a ($\times 10^3$ M s^{-1})	K_d ($\times 10^{-3}$ s^{-1})	K_D ($\times 10^{-7}$)	χ^2
D4 (Aβ40)	135	2.97	0.22	1.68
B6 (Aβ40)	11.6	2.8	2.41	2.82
D4 (Aβ 25−35)	4.79	3.34	6.97	1.98
B6 (Aβ 25−35)	8.65	1.96	2.26	3.15

We assessed the ability of the two selected scFvs to inhibit Aβ42 aggregation using both the ThT binding assay and AFM imaging. When incubated alone, Aβ42 showed the expected time-dependent increase in fluorescence, reaching a plateau value after approximately 50 h (Figure 3). When co-incubated with equimolar D4 or B6, however, Aβ42 aggregation was strongly inhibited (Figure 3). When incubated alone at similar concentrations, D4 and B6 did not increase fluorescence (Figure 3). The Aβ42 sample alone

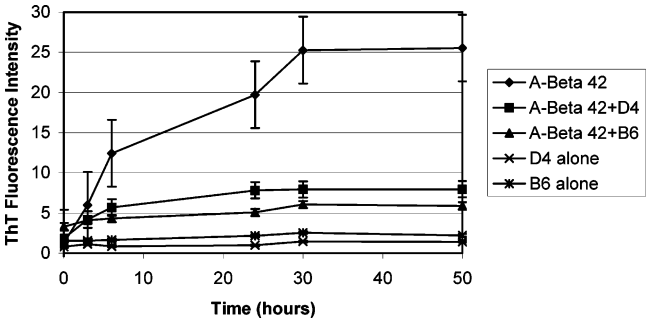

FIGURE 3: Effect of D4 and B6 scFv on aggregation of Aβ42. Aggregation kinetics of Aβ42 was measured alone or in the presence of scFvs D4 and B6, using ThT fluorescence assay. 20 μM Aβ42 alone or with equimolar concentrations of either D4 or B6 was incubated at 37 °C. A 10 μL sample was removed at 0, 3, 6, 24, 30, and 50 h postincubation and added to 2 mL of 5 μM ThT. Fluorescence intensity was measured at an excitation wavelength of 450 nm and emission wavelength of 480 nm.

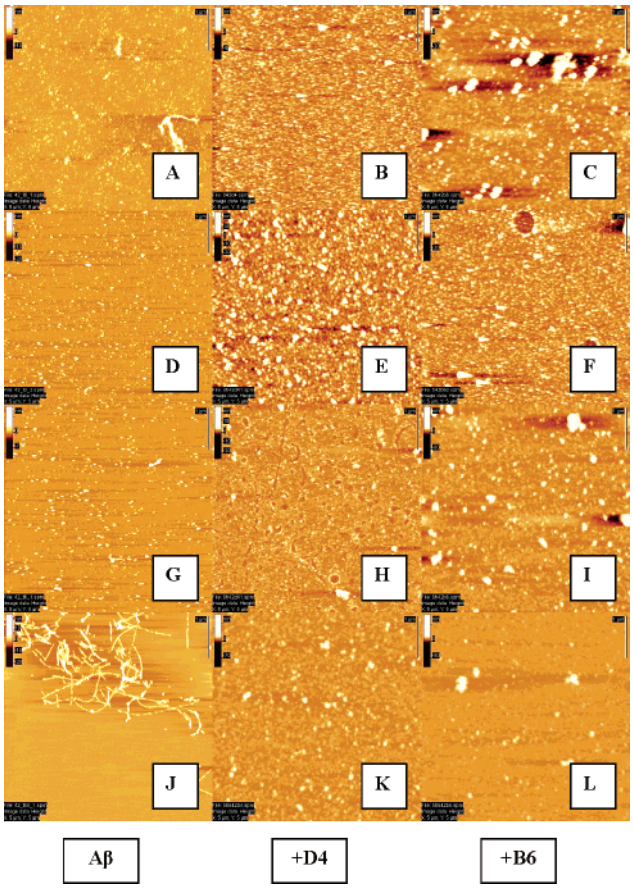

FIGURE 4: AFM images of Aβ42 (20 μM) alone or with equimolar concentrations (20 μM) of D4 and B6 scFvs: Aβ42 alone at 0 h (A), 3 h (D), 6 h (G) and 50 h (J); Aβ42 and D4 scFv at 0 h (B), 3 h (E), 6 h (H), and 50 h (K); Aβ42 and B6 scFv at 0 h (C), 3 h (F), 6 h (I), and 50 h (L).

contained small aggregates at 0 h, forming larger spherical aggregates after 3 and 6 h of incubation and, finally, a mixture of Aβ fibrils and large aggregates after 50 h as visualized by AFM imaging (Figure 4). When Aβ42 was co-incubated with D4 and B6, however, only small aggregates were obtained even after prolonged incubation times (Figure 4), although the B6 sample formed larger aggregates compared to D4. D4 and B6 when incubated alone also

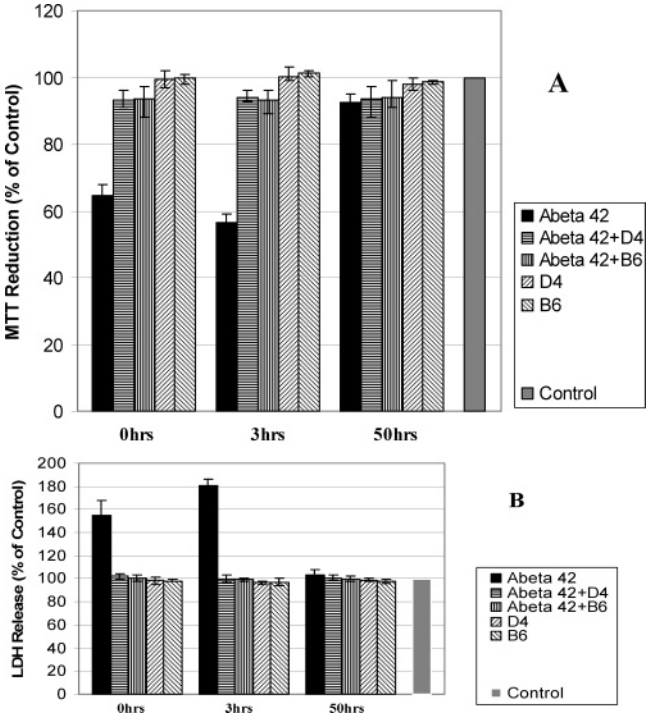

FIGURE 5: Effect of scFv on Aβ42 induced neurotoxicity toward SH-SY5Y human neuroblastoma cells as determined by MTT (A) and LDH (B) assays. 20 μM Aβ42 alone or with equimolar concentrations of either D4 or B6 was incubated at 37 °C. Samples were taken at 0, 3, and 50 h postincubation and added to the cells at a final concentration of 0.5 μM. Cells were incubated with the samples for an additional 48 h before performing MTT reduction assay or LDH release assay. Data shown are mean of three different experiments, and each condition was replicated in six wells for each experiment. Data are expressed as the percentage of control wells containing cells alone.

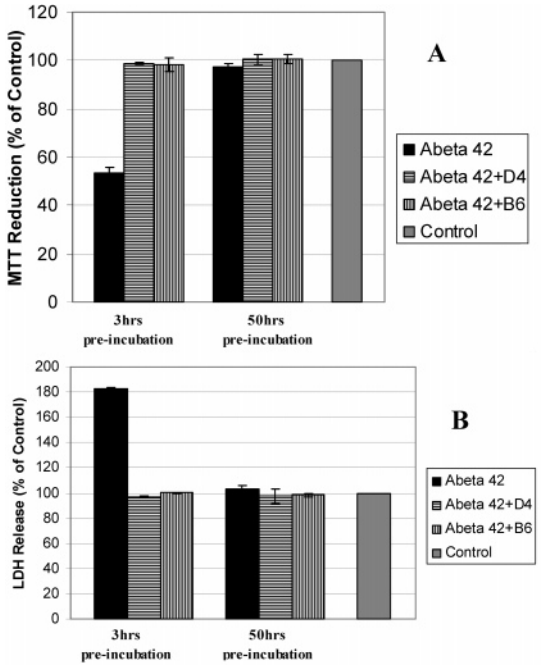

FIGURE 6: Effect of scFv on neurotoxicity toward SH-SY5Y human neuroblastoma cells induced by preincubated Aβ42 as determined by MTT (A) and LDH (B) assays. 20 μM Aβ42 was preincubated for either 3 or 50 h before adding an equimolar concentration of either D4 or B6. For 3 h preincubated Aβ42, samples were incubated for a further 3 h before adding the samples to the cells. For 50 h preincubated Aβ42, samples were incubated for an additional 22 h before addition to the cells. Data shown are the mean of three different experiments and are expressed as a percentage of either MTT reduction or LDH release seen in control wells containing cells alone.

showed aggregate formation in AFM images with B6 again forming larger aggregates than D4 alone (data not shown).

We also tested the ability of the scFvs to inhibit or decrease aggregation from preexisting aggregates by preincubating Aβ42 for either 3 or 50 h before addition of scFv. Addition of B6 or D4 scFvs to the 3 h preincubated sample completely inhibited any further aggregation although neither sample dissolved the preexisting aggregates (data not shown). However, when the B6 or D4 scFvs were added to the 50 h preincubated sample, no inhibition or dissolution of aggregation compared to Aβ42 alone was observed (data not shown). AFM image analyses indicated the presence of small aggregates in the 3 h preincubated samples treated with scFvs and a mixture of large aggregates and fibrils in the 50 h preincubated samples treated with scFvs (data not shown).

Aβ42-induced cytotoxicity toward SH-SY5Y neuroblastoma cells was determined using both MTT toxicity and LDH release assays. Cells treated with aliquots of Aβ42 incubated alone for 0 and 3 h showed reduced MTT activity (Figure 5A) and higher LDH release (Figure 5B) compared to the control wells, indicating toxicity of the small aggregate morphologies of Aβ42. However, cells treated with an aliquot of Aβ42 incubated for 50 h showed little or no toxicity in both MTT and LDH assays, indicating that the later aggregate morphologies observed here are nontoxic to the cells (Figure 5). Addition of either D4 or B6 scFv blocked any Aβ42-induced toxicity at the 0 and 3 h time points and essentially had no effect on 50 h incubated Aβ42 samples (Figure 5).

We also tested whether the scFvs could alter cellular effects of preexisting Aβ aggregates. Aβ42 was incubated alone for either 3 h (small oligomers) or 50 h (large aggregate and fibrils) before addition of equimolar concentrations of D4 and B6 scFv. Both scFvs blocked toxicity of the 3 h sample containing small Aβ42 oligomers, and neither scFv showed any significant effects on 50 h preaggregated Aβ42 samples (Figure 6).

DISCUSSION

The amyloid hypothesis of AD, that Aβ accumulation and deposition in the brain (*50*) leads to neuropathology, has spurred studies on a variety of therapeutic strategies focusing on clearing Aβ in the brain, including very promising active (*35*, *51*, *52*) and passive immunization approaches (*9*, *28*, *29*, *34*, *53*). The mechanisms through which anti-Aβ antibodies reduce Aβ burden and AD pathology, however, are still unclear (*54*). Anti-Aβ antibodies injected intraperitoneally can enter the central nervous system (*34*), possibly through receptor-mediated transport of the Aβ−antibody complex across the blood−brain barrier (*55*), and clear preexisting β-amyloid plaques (*34*). Administration of antibodies against Aβ in transgenic mice models, either peripherally (*34*) or intracranially (*33*), results in widespread activation of microglia, suggesting Fc-mediated mechanisms of amyloid clearance. However, other studies (*36*) have used $F(ab')_2$ fragment and showed reduction in brain Aβ loads, suggesting that non-Fc-mediated processes are also involved. Capture of soluble Aβ in the periphery has also been shown to cause efflux from the central nervous system and reduction

of Aβ deposition in the brain (*9*, *56*). Human Aβ vaccination trials were halted 4 months after initiation when several patients showed signs of aseptic meningoencephalitis (*37*). Despite discontinuation of the trial, several follow-up studies showed that vaccination did lead to production of anti-Aβ antibodies and there was no correlation between the presence of antibodies (*28*) or their titer (*38*) and the incidence and severity of encephalomyelitis. However, an autopsy of an immunized patient (*57*) showed widespread inflammation in the brain, suggesting that, under certain circumstances, an autoimmune, proinflammatory reaction against Aβ can occur (*58*). Several other studies also support the notion of harmful inflammatory responses as a result of immunization strategies (*37*, *39*, *40*). Passive Aβ immunization in a mouse model of AD showed significant reduction of diffuse amyloid but also caused an increase in cerebral microhemorrhages, a possible link to neuroinflammatory complications of Aβ immunization (*40*). Unlike full antibodies, scFvs do not contain the Fc region and therefore should not activate the complement cascade nor microglial cells, two reactions that can lead to excessive inflammation and damage in the brain. Aβ 25−35 is the shortest derivative of Aβ that still forms large β-sheet fibrils, it is highly neurotoxic (*44*, *59*−*62*), and it has been proposed as the most biologically active region of Aβ. Aβ 25−35 is present in senile plaques and degenerating hippocampal neurons in AD brains but not in age-matched control subjects (*45*), and certain forms of Aβ40 can be converted to Aβ 25−35 by brain proteases (*45*). Because of the potential toxicity of this region, we isolated scFvs to the Aβ 25−35 peptide to study as potential noninflammatory therapeutics for AD and show that scFvs to Aβ 25−35 can effectively inhibit aggregation of full-length Aβ42. On the basis of the k_d values, the D4 scFv has higher affinity for Aβ40 compared to B6, whereas B6 has higher affinity for the Aβ 25−35 fragment, suggesting that D4 and B6 may prefer slightly different conformations of Aβ. When incubated alone Aβ42 first forms small spherical aggregates (oligomers) followed by amyloid fibrils as noted in numerous other studies (*22*, *49*, *63*−*65*). When monomeric Aβ42 was co-incubated with either the D4 or B6 scFv, small spherical aggregates were still formed at the early time points, but large fibrillar aggregates were not formed at the later time points. Both scFvs also inhibit further aggregation of preexisting Aβ oligomers, indicating that these scFvs can bind the early Aβ aggregate morphologies. The scFvs did not reduce or dissolve preexisting Aβ fibrillar samples.

The toxicity of the Aβ aggregate samples toward SH-SY5Y cells indicates that the small oligomeric species rather than the large fibrillar aggregates are the toxic morphologies, consistent with numerous other recent studies (*15*, *22*, *66*−*68*). While incubation of Aβ42 with the D4 and B6 scFvs did not prevent formation of small oligomeric aggregates, the scFvs did block the toxic effects of the aggregates. When the scFvs were added to the preexisting small oligomeric species, toxicity of the aggregates was again blocked. On the basis of these results it is likely the scFvs isolated here bind the monomeric and oligomeric forms of Aβ42, preventing further assembly of these species to larger fibrillar aggregates and more importantly preventing the oligomeric species from interacting with the cells and inducing toxic effects. In our studies the Aβ fibril species are not toxic to the SH-SY5Y neuronal cells, in agreement with numerous other studies suggesting that dissolution of Aβ fibrillar plaques may not be a suitable end point for Aβ-based therapeutics.

ScFvs against the Aβ 25−35 fragment can successfully inhibit Aβ42 aggregation and reduce toxicity induced by Aβ42 toward neuronal cells. These scFvs have an added advantage of not having the Fc fragment found in full-sized antibodies, thereby potentially eliminating some of the damaging inflammatory responses associated with full antibodies. The affinity of the scFvs isolated here can be readily improved by affinity maturation for potential therapeutic applications. Other scFvs against full-length Aβ peptide that also inhibit aggregation and reduce toxicity toward neuronal cells have been reported by our laboratory (*22*) and others (*69*, *70*), providing the potential to develop a cocktail of scFvs recognizing a variety of different Aβ regions and morphologies as part of a noninflammatory therapeutic treatment for AD.

REFERENCES

1. Lee, V. M.-Y., Balin, B. J., Otvos, L., Jr., and Trojanowski, J. Q. (1991) A68: A major subunit of paired helical filaments and derivatized forms of normal tau, *Science 251*, 675−678.
2. Forman, M. S., Trojanowski, J. Q., and Lee, V. M. (2004) Neurodegenerative diseases: A decade of discoveries paves the way for therapeutic breakthroughs, *Nat. Med. 10*, 1055−1063.
3. Hebert, L. E., Scherr, P. A., Bienias, J. L., Bennett, D. A., and Evans, D. A. (2003) Alzheimer disease in the US population: Prevalence estimates using the 2000 census, *Arch. Neurol. 60*, 1119−1122.
4. Wancata, J., Musalek, M., Alexandrowicz, R., and Krautgartner, M. (2003) Number of dementia sufferers in Europe between the years 2000 and 2050, *Eur. Psychiatry 18*, 306−313.
5. Selkoe, D. J. (1997) Alzheimer's disease: Genotypes, phenotypes, and treatments, *Science 275*, 630−631.
6. Golde, T. E., Eckman, C. B., and Younkin, S. G. (2000) Biochemical detection of abeta isoforms: Implications for pathogenesis, diagnosis, and treatment of Alzheimer's disease, *Biochim. Biophys. Acta 1502*, 172−187.
7. Goate, A., Chartier-Harlin, M. C., Mullan, M., Brown, J., Crawford, F., Fidani, L., Giuffra, L., Haynes, A., Irving, N., James, L., et al. (1991) Segregation of a missense mutation in the amyloid precursor protein gene with familial Alzheimer's disease, *Nature 349*, 704−706.
8. Kim, T. W., and Tanzi, R. E. (1997) Presenilins and Alzheimer's disease, *Curr. Opin. Neurobiol. 7*, 683−688.
9. DeMattos, R. B., Bales, K. R., Cummins, D. J., Dodart, J. C., Paul, S. M., and Holtzman, D. M. (2001) Peripheral anti-abeta antibody alters CNS and plasma abeta clearance and decreases brain abeta burden in a mouse model of Alzheimer's disease, *Proc. Natl. Acad. Sci. U.S.A. 98*, 8850−8855.
10. Lorenzo, A., and Yankner, B. A. (1994) Beta-amyloid neurotoxicity requires fibril formation and is inhibited by congo red, *Proc. Natl. Acad. Sci. U.S.A. 91*, 12243−12247.
11. Pike, C. J., Walencewicz, A. J., Glabe, C. G., and Cotman, C. W. (1991) Aggregation-related toxicity of synthetic beta-amyloid protein in hippocampal cultures, *Eur. J. Pharmacol. 207*, 367−368.
12. Chromy, B. A., Nowak, R. J., Lambert, M. P., Viola, K. L., Chang, L., Velasco, P. T., Jones, B. W., Fernandez, S. J., Lacor, P. N., Horowitz, P., Finch, C. E., Krafft, G. A., and Klein, W. L. (2003) Self-assembly of abeta(1-42) into globular neurotoxins, *Biochemistry 42*, 12749−12760.
13. Lambert, M. P., Viola, K. L., Chromy, B. A., Chang, L., Morgan, T. E., Yu, J., Venton, D. L., Krafft, G. A., Finch, C. E., and Klein, W. L. (2001) Vaccination with soluble abeta oligomers generates toxicity-neutralizing antibodies, *J. Neurochem. 79*, 595−605.
14. Walsh, D. M., and Selkoe, D. J. (2004) Oligomers on the brain: The emerging role of soluble protein aggregates in neurodegeneration, *Protein Pept. Lett. 11*, 213−228.
15. Cleary, J. P., Walsh, D. M., Hofmeister, J. J., Shankar, G. M., Kuskowski, M. A., Selkoe, D. J., and Ashe, K. H. (2005) Natural

oligomers of the amyloid-beta protein specifically disrupt cognitive function, *Nat. Neurosci. 8*, 79−84.
16. Lue, L. F., Kuo, Y. M., Roher, A. E., Brachova, L., Shen, Y., Sue, L., Beach, T., Kurth, J. H., Rydel, R. E., and Rogers, J. (1999) Soluble amyloid beta peptide concentration as a predictor of synaptic change in Alzheimer's disease, *Am. J. Pathol. 155*, 853−862.
17. McLean, C. A., Cherny, R. A., Fraser, F. W., Fuller, S. J., Smith, M. J., Beyreuther, K., Bush, A. I., and Masters, C. L. (1999) Soluble pool of abeta amyloid as a determinant of severity of neurodegeneration in Alzheimer's disease, *Ann. Neurol. 46*, 860−866.
18. Wang, J., Dickson, D. W., Trojanowski, J. Q., and Lee, V. M. (1999) The levels of soluble versus insoluble brain abeta distinguish Alzheimer's disease from normal and pathologic aging, *Exp. Neurol. 158*, 328−337.
19. Schenk, D., Games, D., and Seubert, P. (2001) Potential treatment opportunities for Alzheimer's disease through inhibition of secretases and abeta immunization, *J. Mol. Neurosci. 17*, 259−267.
20. Frenkel, D., Dewachter, I., Van Leuven, F., and Solomon, B. (2003) Reduction of beta-amyloid plaques in brain of transgenic mouse model of Alzheimer's disease by efrh-phage immunization, *Vaccine 21*, 1060−1065.
21. Liu, R., McAllister, C., Lyubchenko, Y., and Sierks, M. R. (2004) Proteolytic antibody light chains alter beta-amyloid aggregation and prevent cytotoxicity, *Biochemistry 43*, 9999−10007.
22. Liu, R., Yuan, B., Emadi, S., Zameer, A., Schulz, P., McAllister, C., Lyubchenko, Y., Goud, G., and Sierks, M. R. (2004) Single chain variable fragments against beta-amyloid (abeta) can inhibit abeta aggregation and prevent abeta-induced neurotoxicity, *Biochemistry 43*, 6959−6967.
23. Kim, H. D., Kong, F. K., Cao, Y., Lewis, T. L., Kim, H., Tang, D. C., and Fukuchi, K. (2004) Immunization of Alzheimer model mice with adenovirus vectors encoding amyloid beta-protein and GM-CSF reduces amyloid load in the brain, *Neurosci. Lett. 370*, 218−223.
24. Lavie, V., Becker, M., Cohen-Kupiec, R., Yacoby, I., Koppel, R., Wedenig, M., Hutter-Paier, B., and Solomon, B. (2004) Efrh-phage immunization of Alzheimer's disease animal model improves behavioral performance in morris water maze trials, *J. Mol. Neurosci. 24*, 105−113.
25. Jantzen, P. T., Connor, K. E., DiCarlo, G., Wenk, G. L., Wallace, J. L., Rojiani, A. M., Coppola, D., Morgan, D., and Gordon, M. N. (2002) Microglial activation and beta-amyloid deposit reduction caused by a nitric oxide-releasing nonsteroidal anti-inflammatory drug in amyloid precursor protein plus presenilin-1 transgenic mice, *J. Neurosci. 22*, 2246−2254.
26. Schiltz, J. G., Salzer, U., Mohajeri, M. H., Franke, D., Heinrich, J., Pavlovic, J., Wollmer, M. A., Nitsch, R. M., and Moelling, K. (2004) Antibodies from a DNA peptide vaccination decrease the brain amyloid burden in a mouse model of Alzheimer's disease, *J. Mol. Med. 82*, 706−714.
27. Morgan, D., Diamond, D. M., Gottschall, P. E., Ugen, K. E., Dickey, C., Hardy, J., Duff, K., Jantzen, P., DiCarlo, G., Wilcock, D., Connor, K., Hatcher, J., Hope, C., Gordon, M., and Arendash, G. W. (2000) A beta peptide vaccination prevents memory loss in an animal model of Alzheimer's disease, *Nature 408*, 982−985.
28. Hock, C., Konietzko, U., Streffer, J. R., Tracy, J., Signorell, A., Muller-Tillmanns, B., Lemke, U., Henke, K., Moritz, E., Garcia, E., Wollmer, M. A., Umbricht, D., de Quervain, D. J., Hofmann, M., Maddalena, A., Papassotiropoulos, A., and Nitsch, R. M. (2003) Antibodies against beta-amyloid slow cognitive decline in Alzheimer's disease, *Neuron 38*, 547−554.
29. Chauhan, N. B., and Siegel, G. J. (2005) Efficacy of anti-abeta antibody isotypes used for intracerebroventricular immunization in Tgcrnd8, *Neurosci. Lett. 375*, 143−147.
30. Gaugler, M. N., Tracy, J., Kuhnle, K., Crameri, A., Nitsch, R. M., and Mohajeri, M. H. (2005) Modulation of Alzheimer's pathology by cerebro-ventricular grafting of hybridoma cells expressing antibodies against abeta in vivo, *FEBS Lett. 579*, 753−756.
31. Mohajeri, M. H., Saini, K., Schultz, J. G., Wollmer, M. A., Hock, C., and Nitsch, R. M. (2002) Passive immunization against beta-amyloid peptide protects central nervous system (CNS) neurons from increased vulnerability associated with an Alzheimer's disease-causing mutation, *J. Biol. Chem. 277*, 33012−33017.
32. Morgan, D., and Gitter, B. D. (2004) Evidence supporting a role for anti-abeta antibodies in the treatment of Alzheimer's disease, *Neurobiol. Aging 25*, 605−608.
33. Wilcock, D. M., DiCarlo, G., Henderson, D., Jackson, J., Clarke, K., Ugen, K. E., Gordon, M. N., and Morgan, D. (2003) Intracranially administered anti-abeta antibodies reduce beta-amyloid deposition by mechanisms both independent of and associated with microglial activation, *J. Neurosci. 23*, 3745−3751.
34. Bard, F., Cannon, C., Barbour, R., Burke, R. L., Games, D., Grajeda, H., Guido, T., Hu, K., Huang, J., Johnson-Wood, K., Khan, K., Kholodenko, D., Lee, M., Lieberburg, I., Motter, R., Nguyen, M., Soriano, F., Vasquez, N., Weiss, K., Welch, B., Seubert, P., Schenk, D., and Yednock, T. (2000) Peripherally administered antibodies against amyloid beta-peptide enter the central nervous system and reduce pathology in a mouse model of Alzheimer disease, *Nat. Med. 6*, 916−919.
35. Schenk, D., Barbour, R., Dunn, W., Gordon, G., Grajeda, H., Guido, T., Hu, K., Huang, J., Johnson-Wood, K., Khan, K., Kholodenko, D., Lee, M., Liao, Z., Lieberburg, I., Motter, R., Mutter, L., Soriano, F., Shopp, G., Vasquez, N., Vandevert, C., Walker, S., Wogulis, M., Yednock, T., Games, D., and Seubert, P. (1999) Immunization with amyloid-beta attenuates Alzheimer-disease-like pathology in the PDAPP mouse, *Nature 400*, 173−177.
36. Bacskai, B. J., Kajdasz, S. T., McLellan, M. E., Games, D., Seubert, P., Schenk, D., and Hyman, B. T. (2002) Non-fc-mediated mechanisms are involved in clearance of amyloid-beta in vivo by immunotherapy, *J. Neurosci. 22*, 7873−7878.
37. Schenk, D. (2002) Amyloid-beta immunotherapy for Alzheimer's disease: The end of the beginning, *Nat. Rev. Neurosci. 3*, 824−828.
38. Orgogozo, J. M., Gilman, S., Dartigues, J. F., Laurent, B., Puel, M., Kirby, L. C., Jouanny, P., Dubois, B., Eisner, L., Flitman, S., Michel, B. F., Boada, M., Frank, A., and Hock, C. (2003) Subacute meningoencephalitis in a subset of patients with AD after abeta42 immunization, *Neurology 61*, 46−54.
39. Gandy, S., and Walker, L. (2004) Toward modeling hemorrhagic and encephalitic complications of Alzheimer amyloid-beta vaccination in nonhuman primates, *Curr. Opin. Immunol. 16*, 607−615.
40. Pfeifer, M., Boncristiano, S., Bondolfi, L., Stalder, A., Deller, T., Staufenbiel, M., Mathews, P. M., and Jucker, M. (2002) Cerebral hemorrhage after passive anti-abeta immunotherapy, *Science 298*, 1379.
41. Kaneko, I., Morimoto, K., and Kubo, T. (2001) Drastic neuronal loss in vivo by beta-amyloid racemized at ser(26) residue: Conversion of non-toxic [d-ser(26)]beta-amyloid 1-40 to toxic and proteinase-resistant fragments, *Neuroscience 104*, 1003−1011.
42. Monji, A., Utsumi, H., Ueda, T., Imoto, T., Yoshida, I., Hashioka, S., Tashiro, K., and Tashiro, N. (2002) Amyloid-beta-protein (a beta) (25-35)-associated free radical generation is strongly influenced by the aggregational state of the peptides, *Life Sci. 70*, 833−841.
43. Pike, C. J., Walencewicz-Wasserman, A. J., Kosmoski, J., Cribbs, D. H., Glabe, C. G., and Cotman, C. W. (1995) Structure-activity analyses of beta-amyloid peptides: Contributions of the beta 25-35 region to aggregation and neurotoxicity, *J. Neurochem. 64*, 253−265.
44. Liu, R., McAllister, C., Lyubchenko, Y., and Sierks, M. R. (2004) Residues 17-20 and 30-35 of beta-amyloid play critical roles in aggregation, *J. Neurosci. Res. 75*, 162−171.
45. Kubo, T., Nishimura, S., Kumagae, Y., and Kaneko, I. (2002) In vivo conversion of racemized beta-amyloid ([d-ser 26]a beta 1-40) to truncated and toxic fragments ([d-ser 26]a beta 25-35/40) and fragment presence in the brains of Alzheimer's patients, *J. Neurosci. Res. 70*, 474−483.
46. Goletz, S., Christensen, P. A., Kristensen, P., Blohm, D., Tomlinson, I., Winter, G., and Karsten, U. (2002) Selection of large diversities of antiidiotypic antibody fragments by phage display, *J. Mol. Biol. 315*, 1087−1097.
47. Marks, J. D., Hoogenboom, H. R., Bonnert, T. P., McCafferty, J., Griffiths, A. D., and Winter, G. (1991) By-passing immunization. Human antibodies from v-gene libraries displayed on phage, *J. Mol. Biol. 222*, 581−597.
48. Wu, H., Goud, G. N., and Sierks, M. R. (1998) Artificial antibodies for affinity chromatography of homologous proteins: Application to blood clotting proteins, *Biotechnol. Prog. 14*, 496−499.

49. LeVine, H., III (1993) Thioflavine T interaction with synthetic Alzheimer's disease beta-amyloid peptides: Detection of amyloid aggregation in solution, *Protein Sci. 2*, 404−410.
50. Hardy, J., and Selkoe, D. J. (2002) The amyloid hypothesis of Alzheimer's disease: Progress and problems on the road to therapeutics, *Science 297*, 353−356.
51. Das, P., Howard, V., Loosbrock, N., Dickson, D., Murphy, M. P., and Golde, T. E. (2003) Amyloid-beta immunization effectively reduces amyloid deposition in FcRgamma-/- knock-out mice, *J. Neurosci. 23*, 8532−8538.
52. Lemere, C. A., Spooner, E. T., LaFrancois, J., Malester, B., Mori, C., Leverone, J. F., Matsuoka, Y., Taylor, J. W., DeMattos, R. B., Holtzman, D. M., Clements, J. D., Selkoe, D. J., and Duff, K. E. (2003) Evidence for peripheral clearance of cerebral abeta protein following chronic, active abeta immunization in PSAPP mice, *Neurobiol. Dis. 14*, 10−18.
53. Du, Y., Wei, X., Dodel, R., Sommer, N., Hampel, H., Gao, F., Ma, Z., Zhao, L., Oertel, W. H., and Farlow, M. (2003) Human anti-beta-amyloid antibodies block beta-amyloid fibril formation and prevent beta-amyloid-induced neurotoxicity, *Brain 126*, 1935−1939.
54. Broytman, O., and Malter, J. S. (2004) Anti-abeta: The good, the bad, and the unforeseen, *J. Neurosci. Res. 75*, 301−306.
55. Poduslo, J. F., and Curran, G. L. (2001) Amyloid beta peptide as a vaccine for Alzheimer's disease involves receptor-mediated transport at the blood-brain barrier, *Neuroreport 12*, 3197−3200.
56. Dodart, J. C., Bales, K. R., Gannon, K. S., Greene, S. J., DeMattos, R. B., Mathis, C., DeLong, C. A., Wu, S., Wu, X., Holtzman, D. M., and Paul, S. M. (2002) Immunization reverses memory deficits without reducing brain abeta burden in Alzheimer's disease model, *Nat. Neurosci. 5*, 452−457.
57. Nicoll, J. A., Wilkinson, D., Holmes, C., Steart, P., Markham, H., and Weller, R. O. (2003) Neuropathology of human Alzheimer disease after immunization with amyloid-beta peptide: A case report, *Nat. Med. 9*, 448−452.
58. Munch, G., and Robinson, S. R. (2002) Alzheimer's vaccine: A cure as dangerous as the disease?, *J. Neural Transm. 109*, 537−539.
59. Butterfield, D. A., Martin, L., Carney, J. M., and Hensley, K. (1996) A beta (25-35) peptide displays H_2O_2-like reactivity towards aqueous Fe^{2+}, nitroxide spin probes, and synaptosomal membrane proteins, *Life Sci. 58*, 217−228.
60. Misiti, F., Sampaolese, B., Pezzotti, M., Marini, S., Coletta, M., Ceccarelli, L., Giardina, B., and Clementi, M. E. (2005) Abeta-(31-35) peptide induce apoptosis in PC 12 cells: Contrast with abeta(25-35) peptide and examination of underlying mechanisms, *Neurochem. Int. 46*, 575−583.
61. Olariu, A., Tran, M. H., Yamada, K., Mizuno, M., Hefco, V., and Nabeshima, T. (2001) Memory deficits and increased emotionality induced by beta-amyloid (25-35) are correlated with the reduced acetylcholine release and altered phorbol dibutyrate binding in the hippocampus, *J. Neural Transm. 108*, 1065−1079.
62. Perez, M., Cuadros, R., Benitez, M. J., and Jimenez, J. S. (2004) Interaction of Alzheimer's disease amyloid beta peptide fragment 25-35 with tau protein, and with a tau peptide containing the microtubule binding domain, *J. Alzheimer's Dis. 6*, 461−467.
63. Ghanta, J., Shen, C. L., Kiessling, L. L., and Murphy, R. M. (1996) A strategy for designing inhibitors of beta-amyloid toxicity, *J. Biol. Chem. 271*, 29525−29528.
64. LeVine, H., III (1997) Stopped-flow kinetics reveal multiple phases of thioflavin t binding to Alzheimer beta (1-40) amyloid fibrils, *Arch. Biochem. Biophys. 342*, 306−316.
65. Legleiter, J., Czilli, D. L., Gitter, B., DeMattos, R. B., Holtzman, D. M., and Kowalewski, T. (2004) Effect of different anti-abeta antibodies on abeta fibrillogenesis as assessed by atomic force microscopy, *J. Mol. Biol. 335*, 997−1006.
66. Glabe, C. C. (2005) Amyloid accumulation and pathogensis of Alzheimer's disease: Significance of monomeric, oligomeric and fibrillar abeta, *Subcell. Biochem. 38*, 167−177.
67. Klyubin, I., Walsh, D. M., Lemere, C. A., Cullen, W. K., Shankar, G. M., Betts, V., Spooner, E. T., Jiang, L., Anwyl, R., Selkoe, D. J., and Rowan, M. J. (2005) Amyloid beta protein immunotherapy neutralizes abeta oligomers that disrupt synaptic plasticity in vivo, *Nat. Med. 11*, 556−561.
68. Walsh, D. M., Townsend, M., Podlisny, M. B., Shankar, G. M., Fadeeva, J. V., Agnaf, O. E., Hartley, D. M., and Selkoe, D. J. (2005) Certain inhibitors of synthetic amyloid beta-peptide (abeta) fibrillogenesis block oligomerization of natural abeta and thereby rescue long-term potentiation, *J. Neurosci. 25*, 2455−2462.
69. Manoutcharian, K., Acero, G., Munguia, M. E., Montero, J. A., Govezensky, T., Cao, C., Ugen, K., and Gevorkian, G. (2003) Amyloid-beta peptide-specific single chain fv antibodies isolated from an immune phage display library, *J. Neuroimmunol. 145*, 12−17.
70. Manoutcharian, K., Acero, G., Munguia, M. E., Becerril, B., Massieu, L., Govezensky, T., Ortiz, E., Marks, J. D., Cao, C., Ugen, K., and Gevorkian, G. (2004) Human single chain Fv antibodies and a complementarity determining region-derived peptide binding to amyloid-beta 1-42, *Neurobiol. Dis. 17*, 114−121.

BI060601O